Stream-groundwater exchange and hydrologic turnover at the network scale

Tim Covino,[1] Brian McGlynn,[1] and John Mallard[1]

Received 19 May 2011; revised 16 September 2011; accepted 2 November 2011; published 16 December 2011.

[1] The exchange of water between streams and groundwater can influence stream water quality, hydrologic mass balances, and attenuate solute export from watersheds. We used conservative tracer injections (chloride, Cl^-) across 10 stream reaches to investigate stream water gains and losses from and to groundwater at larger spatial and temporal scales than typically associated with hyporheic exchanges. We found strong relationships between reach discharge, median tracer velocity, and gross hydrologic loss across a range of stream morphologies and sizes in the 11.4 km^2 Bull Trout Watershed of central ID. We implemented these empirical relationships in a numerical network model and simulated stream water gains and losses and subsequent fractional hydrologic turnover across the stream network. We found that stream gains and losses from and to groundwater can influence source water contributions and stream water compositions across stream networks. Quantifying proportional influences of source water contributions from runoff generation locations across the network on stream water composition can provide insight into the internal mechanisms that partially control the hydrologic and biogeochemical signatures observed along networks and at watershed outlets.

Citation: Covino, T., B. McGlynn, and J. Mallard (2011), Stream-groundwater exchange and hydrologic turnover at the network scale, *Water Resour. Res.*, *47*, W12521, doi:10.1029/2011WR010942.

1. Introduction

[2] The bidirectional movement of water between streams and groundwater (GW) has been implicated as exerting important controls over hydrological and biogeochemical processes. Increasingly, it is being recognized that stream reaches typically do not only gain or lose water along a reach (e.g., $\geq$100 m), as indicated by net changes in discharge (Q), but that dynamic gross hydrologic gains from and losses to GW systems often occur over a wide range of net Q [*Covino and McGlynn*, 2007; *Covino et al.*, 2010; *Payn et al.*, 2009; *Ruehl et al.*, 2006; *Schmadel et al.*, 2010; *Story et al.*, 2003]. This indicates that exchanges of water between streams and GW may be difficult to elucidate based solely on net changes in Q [*Szeftel et al.*, 2011]. However, accurate assessment of stream-GW exchange is important because the bidirectional movement of water into and out of stream channels can exert substantial controls over solute transport [*Ren and Packman*, 2005], stream solute composition [*Covino and McGlynn*, 2007], aquifer recharge [*Ruehl et al.*, 2006], the spatial sources of streamflow [*McGlynn and Seibert*, 2003], and biological nutrient uptake and retention processes [*Covino et al.*, 2010; *Mulholland et al.*, 1997].

[3] Exchanges of water between streams and GW occur across a range of temporal and spatial scales [e.g., *Cardenas*, 2008; *Woessner*, 2000]. Smaller scale exchanges, often documented in hyporheic studies, typically occur over spatial scales of centimeters and temporal scales of minutes [*Harvey et al.*, 1996]. Conversely, larger-scale exchanges between streams and GW can occur over hundreds to thousands of meters and time scales of years [*Harvey et al.*, 1996]. Across a mountain to valley transition over a spatial scale of $\sim$1 km in the Centennial Mountains of Montana, *Covino and McGlynn* [2007] found up to 66% gross loss and 32% gross gain resulting in net streamflow changes of (−)34%. Furthermore, *Covino and McGlynn* [2007], *Payn et al.* [2009], and *Covino et al.* [2010] each noted concurrent gains and losses along numerous stream reaches, including those with little net change in Q, and highlighted the importance of quantifying the water balance components that constitute net changes in Q along stream reaches. While these larger-scale hydrologic exchanges have been noted as important for controlling water balances [*Payn et al.*, 2009], informing transient storage and exchange estimates [*Szeftel et al.*, 2011], influencing nutrient transport [*Covino et al.*, 2010], and controlling stream water solute composition and aquifer storage state [*Covino and McGlynn*, 2007], they remain poorly understood, inadequately incorporated into stream network models, and not previously assessed for their integrated affect on watershed outlet source water compositions.

[4] Stream gains from and losses to GW are spatially organized by watershed structure and stream network geometry. Watershed structure, or the spatial arrangement of convergent and divergent hillslopes, organizes the delivery of water to the channel network. Stream network geometry, or the spatial arrangement of stream segments, organizes the paths traveled to the watershed outlet. Strong gains

[1]Department of Land Resources and Environmental Sciences, Montana State University, Bozeman, Montana, USA.

0043-1397/11/2011WR010942

(i.e., greater lateral inflows of water) often occur along stream reaches with large lateral watershed area or upslope-accumulated area (UAA) compared to regions with smaller UAA [*Jencso et al.*, 2009]. After water enters the channel network, streamflow gains and losses from and to GW can lead to changing stream water composition moving downstream, a process we refer to as fractional hydrologic turnover. We define hydrologic turnover as the process of streams losing a fraction of water to GW while sequentially or simultaneously receiving different water from GW. This process can lead to changing stream water composition and diminishes the influence of any one particular GW input moving downstream. For example, water that enters the channel network near the headwaters (i.e., channel heads) will initially impart a strong influence on stream water composition; however, this influence or signature will subsequently decay with distance traveled downstream due to stream-GW exchange and hydrologic turnover (i.e., loss of some of the original input and gain of different water). Therefore, both watershed structure, which organizes lateral inflows to the network, and network geometry, which influences distance traveled along the network, can exert important controls over stream water composition and solute signatures observed along stream networks and at watershed outlets. Indeed, many researchers have used either watershed outlet or stream network synoptic sampling-based information to infer internal watershed processes. Here we seek to elucidate the roles of watershed structure, network geometry, and hydrologic turnover in influencing signals observed along stream networks and at watershed outlets to better inform inferences made from stream water measures.

[5] We quantified gross gains, gross losses, and net changes in Q using a consecutive tracer approach across 10 stream reaches that span the range of reach types (first–third order), watershed area (0.2–11.4 km^2), discharge (0.8–730.4 L s^{-1}), and geomorphologies (steep headwater to alluvial valley bottom) across the stream network. Based on observed experimental data, we developed a stream network model of hydrologic turnover to assess the role of watershed structure and stream network geometry in influencing source water contributions, and stream water composition along the ~14 km stream network in the Bull Trout Watershed, central ID (~11.4 km^2). We address the following questions with our combined experimental and model based investigation:

[6] 1. How do magnitudes of reach scale stream-GW exchange vary across the stream network?

[7] 2. How do observed reach-scale stream-GW exchange and hydrologic turnover processes combine to influence source water contributions and stream water composition at the network scale?

2. Methods

[8] We performed conservative tracer (chloride, Cl^-) injections on 10 stream reaches within the Bull Trout Watershed in the Sawtooth Mountains of central Idaho to quantify net changes in Q and gross hydrologic exchanges between stream water and GW along each reach (Figure 1). We used the results of these experiments to develop a numerical network model, parameterized with empirical measurements, that simulates hydrologic gains, losses, and turnover across the Bull Trout stream network.

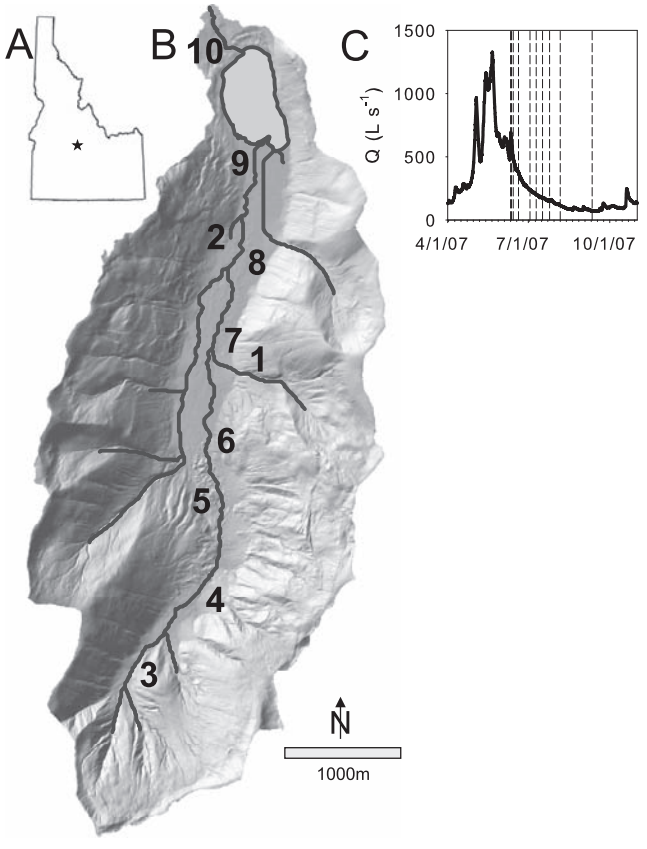

Figure 1. (a) Location of the Bull Trout Watershed in the Sawtooth Mountains of central Idaho. (b) Detailed map of the watershed and locations of the 10 experimental stream reaches. Stream reaches are ordered by increasing watershed area (i.e., reach 10 has the largest watershed area). (c) Hydrograph and timing of tracer experiments for context.

2.1. Study Area

[9] The Bull Trout Watershed drains an area of 11.4 km^2 and forms the headwaters of the Payette River drainage. Parent lithology in the watershed is biotite granodiorite of the Idaho Batholith, and valley bottom fill is composed of mixed Pleistocene till and Holocene alluvium and colluvium [*Kiilsgaard et al.*, 2003]. Land cover surrounding headwater streams is dominated by lodgepole pine (*Pinus contorta*) while land cover in the valley bottom is dominated by sedges (*Carex* spp.), grasses, and willows (*Salix* spp.). Thirty year average annual precipitation is 108 cm, with 64% in the form of snowfall (Banner Summit snowpack telemetry, SNOTEL, #312, 2140 m elevation, located <2 km from Bull Trout Watershed). Our 10 experimental reaches spanned the continuum of reach characteristics across the stream network, from small headwater to larger valley bottom watershed outlet streams, with stream reach contributing areas ranging between 0.2 and 11.4 km^2 (Figure 1, Table 1). Across the 10 stream reaches, sinuosity ranged from 1.1 to 1.8, stream slope varied between 0.7% and 29.3%, median pebble size (i.e., D_{50}) was 8.0–28.5 mm, and Q ranged from 0.8 to 730.4 L s^{-1}. Sinuosity increased and slope decreased moving in the downstream direction, while pebble size (D_{50}) was variable but did not

Table 1. Summary Information of Reach Characteristics and Tracer Experiment Results

Date	Reach Number	Watershed Area (km^2)	Reach Length (m)	$Q_{(i-1)}$ (L s^{-1})	$Q_{(i)}$ (L s^{-1})	Net Change in Q (L s^{-1} 100 m^{-1})	Gross Gain (L s^{-1} 100 m^{-1})	Gross Loss (L s^{-1} 100 m^{-1})	Median Tracer Velocity (m h^{-1})
24 Jul 06	1	0.20	450	11.3	9.7	−0.34	0.67	−1.01	676.8
6 Aug 07	1	0.20	200	4.4	3.6	−0.40	0.21	−0.61	478.1
25 Jul 07	2	0.27	191	1.9	0.8	−0.57	0.18	−0.74	284.4
23 Sep 06	3	0.62	200	3.4	2.5	−0.45	0.63	−1.08	138.2
11 Sep 07	3	0.62	225	2.3	2.5	0.08	0.83	−0.75	139.7
7 Aug 06	4	2.31	400	14.9	34.2	4.83	6.05	−1.22	691.2
17 Jul 07	4	2.31	385	17.3	29.6	3.19	3.82	−0.63	669.6
20 Jul 06	5	4.41	500	132.8	174.4	8.32	11.03	−2.71	1296.0
10 Jul 07	5	4.41	800	78.2	109.6	3.93	5.49	−1.56	957.6
14 Jun 07	6	7.50	1050	197.0	284.0	8.29	19.17	−10.88	684.0
14 Jun 07	7	8.82	2246	284.0	316.0	1.42	7.37	−5.94	831.6
3 Jul 07	7	8.82	491	87.9	96.2	1.69	4.38	−2.69	633.6
12 Jun 07	8	9.43	1000	372.7	366.4	−0.63	15.88	−16.51	1098.0
14 Jun 07	9	9.49	3744	316.0	328.0	0.32	1.42	−1.10	889.2
11 Jun 07	10	11.39	500	712.0	730.4	3.68	9.38	−5.70	1008.0
20 Jun 07	10	11.39	550	501.5	449.9	−9.38	1.56	−10.94	741.6

follow a clear trend. We performed tracer experiments during the months of June–September of 2006 and 2007.

2.2. Determining Net Changes in Discharge Across the Stream Reaches

[10] We performed dilution gauging to measure Q first at the downstream (base) and second at the upstream (head) endpoints along each of 10 stream reaches. We dissolved sodium chloride (NaCl) in stream water and injected it as an instantaneous (i.e., slug) injection at appropriate mixing lengths upstream of the sampling location (12–50 m). We confirmed appropriate mixing lengths immediately preceding the Cl^- injections by adding fluorescent Rhodamine-WT to the stream and observing complete mixing. During each Cl^- dilution gauging injection, we measured real-time specific conductance (SC) with Campbell Scientific CS547A conductivity and temperature probes connected to Campbell Scientific data loggers (Logan, UT). Conductivity probes were secured at mid-depth of the thalweg and SC data were collected every 2 s prior to tracer arrival (i.e., background concentration without the influence of added tracer), through tracer arrival (i.e., breakthrough curve, BTC), and after the stream returned to background concentration. Next, we quantified the linear relationship between SC and Cl^- concentration ($r^2 > 0.99$, $p < 0.0001$) and used this relationship to calculate Q from Cl^--BTCs as

$$Q = \frac{T_{\mathrm{MA}}}{\int_0^t T_C(t)dt}, \tag{1}$$

where T_{MA} is the tracer mass added to the stream, and T_C is the background corrected tracer concentration. This approach requires adequate mixing lengths and negligible tracer loss [*Kilpatrick and Cobb*, 1985]; these requirements were satisfied here by stream reaches whose length was optimized to ensure complete mixing while minimizing loss of tracer from the stream. We then determined the net change in Q across the stream reaches as

$$\mathrm{Net}\Delta Q = Q_i - Q_{i-1}, \tag{2}$$

where $\mathrm{Net}\Delta Q$ is the net change in Q across the stream reach, Q_i is Q at the base of the reach, and Q_{i-1} is Q at the head of the reach. Finally we normalized all of the $\mathrm{Net}\Delta Q$ values to changes per 100 m of stream reach to account for differences in total reach lengths.

2.3. Determining Gross Hydrologic Gains and Losses Across the Stream Reaches

[11] Previous research has shown that streams do not simply gain or lose water and associated solutes across their reaches, but that $\mathrm{Net}\Delta Q$ is the result of simultaneous or sequential gross gains and losses occurring along stream reaches [*Covino and McGlynn*, 2007; *Covino et al.*, 2010; *Payn et al.*, 2009]. In contrast to the dilution gauging experiments described above that were performed over short mixing lengths (12–50 m) to ensure negligible tracer loss, we quantified losses that occurred between the head and base of longer stream reaches (191–3744 m total length, see Table 1). Once fully mixed, conservative tracer transport reflects hydrological dynamics, and the amount of tracer loss along each of the stream reaches was used to estimate gross hydrologic loss across each reach. In these mass recovery experiments we injected Cl^- at the head of the stream reach and determined Cl^- mass recovered at the base of the reach (191–3744 m downstream, see Table 1). Tracer mass recovery (T_{MR}) at the base of each reach was calculated as the product of local Q (equation (1)) and the time integrated tracer concentration generated from the tracer injection at the head of the reach (equation (3)),

$$T_{\mathrm{MR}} = Q\int_0^t T_C(t)dt, \tag{3}$$

and tracer loss (T_L) is equal to T_{MA} minus T_{MR}. T_L was calculated in units of mass, but can be converted to fractional or % loss by dividing by T_{MA}, which we refer to as %Loss. Hydrologic gross loss (Q_{LOSS}) is equal to the product of %Loss and Q_{i-1}, and gross gain (Q_{GAIN}) was calculated through mass balance using (equation (4))

$$Q_{\mathrm{GAIN}} = \mathrm{Net}\Delta Q + Q_{\mathrm{LOSS}}. \tag{4}$$

We normalized the Q_{LOSS} and Q_{GAIN} data to changes per 100 m of stream reach in order to account for differences in total reach lengths. For both the Q measurements and mass recovery injections, we determined median tracer velocities as stream distance divided by the time to center of recovered tracer mass. Also, on 6 of the 10 stream reaches (reaches: 1, 3, 4, 5, 7, and 10) we repeated the mass recovery experiments at different flow states to determine how Q_{LOSS} and exchange dynamics varied with Q. Finally, we performed these mass recovery experiments using both instantaneous (i.e., slug) and continuous (i.e., steady state) injections to determine whether the duration of the tracer injection impacted the magnitude of mass recovery.

2.4. Empirical Relationships for Network Model

[12] We measured the hydrologic variables described above (i.e., NetΔQ, Q_{GAIN}, and Q_{LOSS}) on 10 reaches distributed across the stream network (Figure 1). The 10 reaches represent the spectrum of hydrogeomorphic settings (i.e., the physical environment that influences water movement) across the Bull Trout stream network. Based on these sites and experimental results, we quantified empirical relationships between watershed area and Q, Q and Q_{LOSS}, Q and median tracer velocity, and median tracer velocity and Q_{LOSS}.

2.5. Network-Scale Terrain Analysis and Modeling

[13] We implemented the empirical relationships described above within a network scale numerical model to simulate hydrologic gains, losses, and hydrologic turnover across the Bull Trout stream network.

2.5.1. Terrain Analysis

[14] We performed terrain analysis using a combination of digital elevation models (DEMs) derived from 1 m airborne laser swath mapping (ALSM) including a watershed DEM resampled from 1 to 10 m resolution and global positioning system (GPS)-surveyed streamlines. ALSM data were collected on 2 September 2009 by the National Center for Airborne Laser Mapping (NCALM). Instrument vertical accuracy was 5–30 cm and horizontal accuracy 10 cm. Streamlines were surveyed during July–August 2008 using a Trimble GeoXT GPS and subsequently differentially corrected using the Payette National Forest base station ~120 km away in McCall, ID.

[15] Prior to watershed delineation, we applied a drainage-route deepening algorithm on the unclipped DEM (extending beyond the study area) to eliminate sinks in the relatively flat valley bottoms. We delineated the watershed using a single flow direction algorithm [D8, *O'Callaghan and Mark*, 1984]. Contributing area at each watershed cell was calculated using a triangular multiple flow-direction algorithm (MD°) [*Seibert and McGlynn*, 2007] to route flow until the stream channel initiation threshold of 20 ha was reached, after which flow was routed downstream using a single flow direction algorithm [D8, *O'Callaghan and Mark*, 1984]. GPS streamlines and the 1 m ALSM DEM were used to verify and adjust the terrain analysis-derived stream network coverage. Minor, manual terrain modifications were made based on the auxiliary information to correct unrealistic flow paths along the stream network. In addition to the stream network and contributing area to each cell across the watershed, we calculated watershed area for each 10 m cell of the stream network (i.e., stream reach) and the lateral contributing area to each stream reach [*Grabs et al.*, 2010]. We define a stream reach as a 10 m cell within the stream network.

2.5.2. Network Model

[16] Our numerical stream network model is based on a conceptual model of stream reach behavior in which each stream reach (i.e., 10 m stream network cell) receives inputs of discharge from the upstream reach in the stream network and lateral GW inputs from the watershed area flowing directly into that reach (i.e., UAA). In addition to these stream discharge increases (i.e., gains) each reach simultaneously loses some percentage of water to the GW system (Figure 2). The resulting streamflow in each reach then becomes an input to the next downstream reach. These simultaneous gains and losses to and from each reach in the stream network result in fractional turnover of stream water in the downstream direction, where the water in each stream reach is composed of a decayed mixture of water from all upstream reaches (Figure 2).

[17] Flow was initiated as a function of area in the headwater reaches at a threshold of 20 ha. Net gain in each reach was subsequently calculated as a function of the increase in watershed area at that stream reach (i.e., UAA) and does not include Q from upstream reaches. Gross loss to GW was calculated as a function of discharge in the upstream reach based on the empirical relationship between Q and Q_{LOSS} described in section 2.4. Gross gain (Q_{GAIN}) was calculated using the mass balance shown in equation (4). Discharge in reach i was calculated as the balance of the

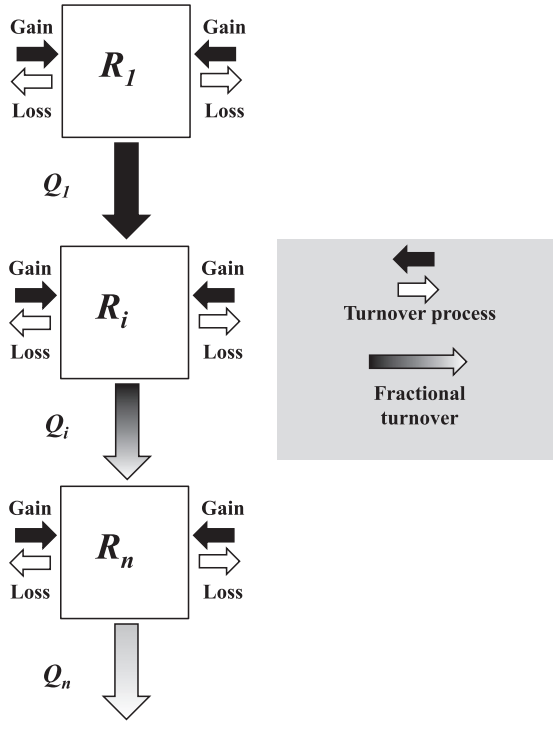

Figure 2. Conceptual model of gross gains and losses, resulting discharge from each reach, and hydrologic turnover, or the fractional turnover process for three hypothetical reaches along the stream network.

input from the upstream reach and the gross gain and loss across reach i (equation (5)),

$$Q_i = Q_{i-1} + Q_{\mathrm{GAIN}} - Q_{\mathrm{LOSS}}. \quad (5)$$

Fractional hydrologic turnover occurs as a result of stream water loss to GW and simultaneous gain of different water from GW across the stream network, and leads to changing stream water composition moving downstream (Figure 2). We calculated the changing stream water composition as the amount of water contributed to reach i by an upstream reach j ($Q_{i,j}$). Mathematically this is the product of the contribution to stream water in reach $i-1$ from reach j, and the proportional contribution to stream water in reach i from all upstream reaches,

$$Q_{i,j} = Q_{i-1,j}\frac{Q_i - Q_{\mathrm{GAIN},i}}{Q_i}. \quad (6)$$

Where $Q_{i-1,j}$ is the stream water contribution to reach $i-1$ from reach j, and $\frac{Q_i - Q_{\mathrm{GAIN},i}}{Q_i}$ is the proportional contribution to Q_i from all upstream reaches. For each reach i across the stream network this equation was applied iteratively moving downstream along all upstream reaches resulting in a distribution of proportional contributions to Q_i from upstream reaches. Headwater reaches were omitted from these calculations as they lack contributions from upstream reaches.

3. Results

3.1. Stream Discharge, Gross Gains and Losses, and Net Changes in Discharge

[18] Q at the head and base of each stream reach (Figures 3a–3c) ranged from 0.8 to 730.4 L s^{-1} (Figure 3a, Table 1), and from 0.010 to 0.223 mm h^{-1} (Figure 3b). Q at the base of each reach was 42%–171% of Q at the head of each stream reach (Figure 3c, note Q at the head of the reach was always 100%). Q is presented in three different units because each highlights different patterns and processes occurring across the network. The L s^{-1} data are indicative of volumetric differences in Q, the mm h^{-1} data reflect hydrologic patterns normalized for watershed area, and the % values indicate changes in Q relative to an initial value at the head of the reach (Figure 3).

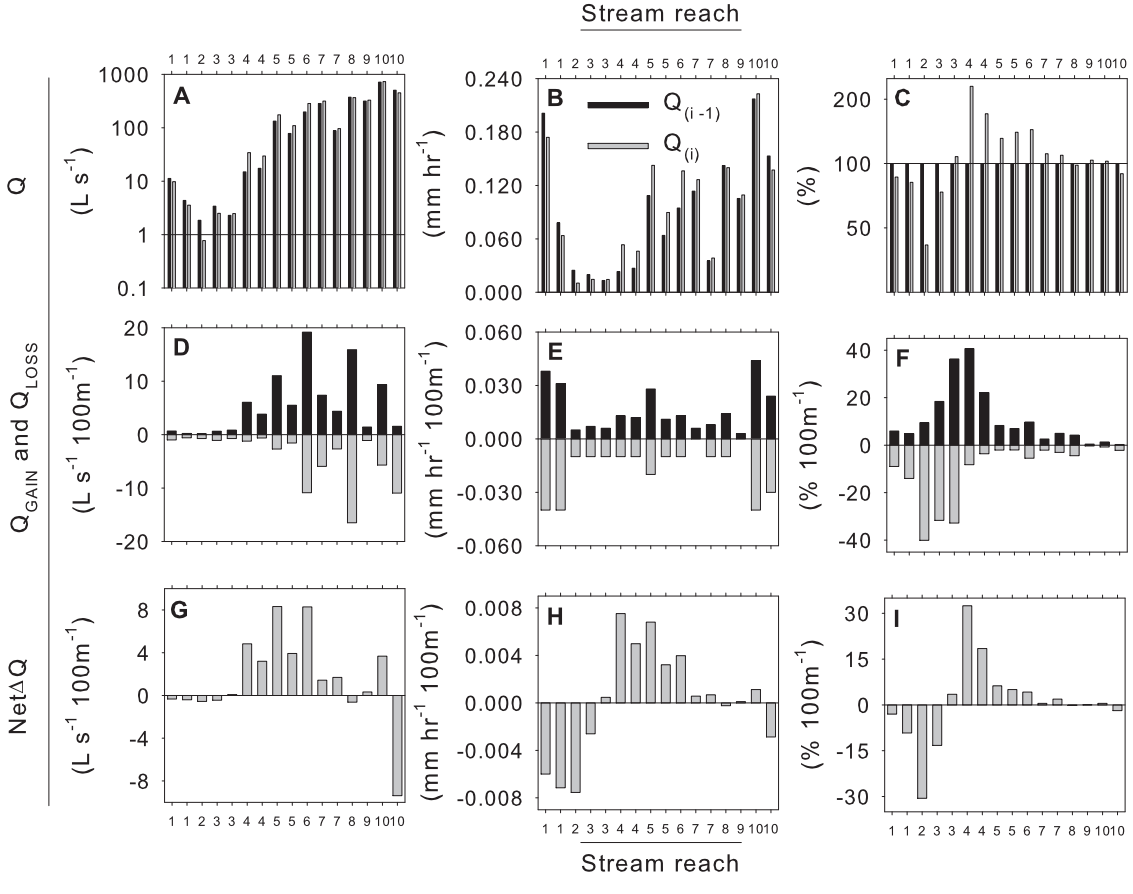

Figure 3. Stream discharge (Q) at the upstream (head) and downstream (base) endpoints of the 10 experimental stream reaches in units of (a) liters per second, (b) millimeters per hour, and (c) percent of upstream Q; (d)–(f) gross gains and losses per 100 m of stream reach in three sets of units; and (g)–(i) net changes in Q that result from gross gains and losses across each reach. Stream reaches are ordered by increasing watershed area (i.e., reach 10 has the largest watershed area), and 6 of the 10 reaches include repeat experiments.

[19] Each set of units was also useful for examining gross hydrologic gains and losses (Figures 3d–3f). Volumetric gains ranged between 0.18 and 19.17 L s^{-1} 100 m^{-1}, and volumetric losses varied between 0.61 and 16.51 L s^{-1} 100 m^{-1} (Figure 3d). Greatest volumetric gains and losses occurred across stream reaches 6, 7, 8, and 10 (note stream reaches listed in order of increasing watershed area), indicating greatest volumetric exchange in medium to larger size streams (Figure 3d). Normalized for watershed area, gross gains ranged from 0.003 to 0.044 mm h^{-1} 100 m^{-1}, and gross losses were between 0.003 and 0.043 mm h^{-1} 100 m^{-1} (Figure 3e). Gross gains and losses normalized for watershed area were greatest at the smallest (reach 1) and largest (reach 10) stream sizes (Figure 3e). Gross gains as a % change per 100 m relative to Q at the head of the reach ranged from 0.3% to 36.3% 100 m^{-1}, and gross losses were 0.4%–40.1% 100 m^{-1} (Figure 3f). The % gains and losses indicate yet another pattern where the greatest % gains and losses occurred on reaches 1–4, and subsequently % gains and losses decreased with increasing watershed area (Figure 3f).

[20] Volumetric net changes in Q (NetΔQ) across the reaches varied between (−)9.38 and (+)8.29 L s^{-1} 100 m^{-1} (Figure 3g). Reaches 4–7 were net gaining, reach 10 was strongly losing during one time point and gaining during another (Figure 3g, Table 1), and the remaining reaches were approximately zero net change despite gross gains and losses (Figures 3d and 3g). Area normalized NetΔQ ranged from (−)0.008 to (+)0.005 mm h^{-1} 100 m^{-1}. Strong losses were measured on reaches 1 and 2, strong gains on reaches 4–6, intermediate losses on reaches 3 and 10, and net changes near zero on the remaining reaches (Figure 3h). The % net changes ranged from (−)30.6 to (+)18.5% 100 m^{-1}, and strongest % net changes were measured on the smaller reaches (i.e., 1–4) and % changes decreased with increasing watershed area (Figure 3i).

[21] We calculated percent tracer mass recovery, using both slug (instantaneous) and steady state (continuous) injection techniques to determine the influence of duration of release on mass recovery. The linear regression between mass recovery estimates obtained from the two approaches for the same reach during the same time period demonstrates that there was no systematic bias in mass recovery calculated using either method (Figure 4). This relationship indicates that similar mass recovery estimates would have been obtained from either approach and that mass recovery was not time dependent at this scale in this case study.

3.2. Empirical Relationships Implemented in the Stream Network Numerical Model

[22] We quantified empirical stream-GW exchange relationships from the stream tracer tests and implemented them in a numerical network model of gross gains, losses, and resulting hydrologic turnover. The linear relationship between watershed area and Q (Figure 5a) was used to estimate NetΔQ for each reach in the network. The relationship between Q_{LOSS} (% 100 m^{-1}) and mean reach Q, defined as the average of upstream and downstream Q across the reach, followed a negative power law (Figure 5b), and was used to estimate Q_{LOSS} across each reach in the stream network. Repeated mass recovery tracer experiments at different flow states along 6 of the 10 stream reaches indicated that loss dynamics varied temporally

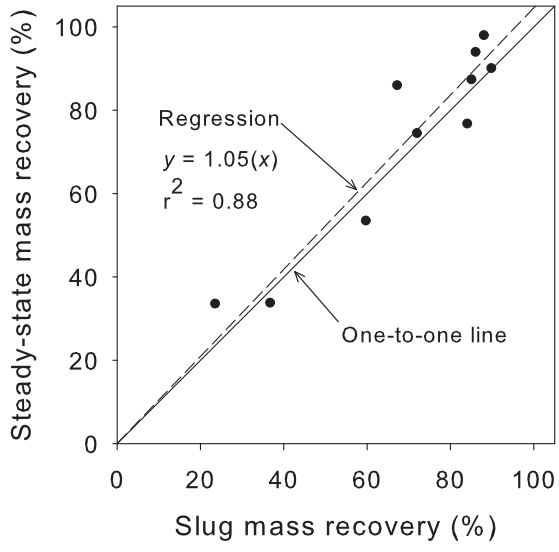

Figure 4. Linear regression relationship between percent mass recovery calculated from instantaneous (i.e., slug) and steady state (i.e., constant-rate) tracer injections performed on the same stream reach during the same time period (i.e., either same day or within one day).

with stream discharge and Q_{LOSS} (% 100 m^{-1}), decreased with increasing Q (Figure 5b). Gross gain (Q_{GAIN}) was calculated using the water balance equation (4) and stream discharge across the reach of interest and (Q_i) was calculated with equation (5). This modeling framework results in net gaining reaches (model results presented in section 3.4) to maintain water balance because watershed area increases in the downstream direction.

[23] We present the relationships between mean reach Q and median tracer velocity (Figure 5c), and median tracer velocity and Q_{LOSS} (Figure 5d) to provide context for interpreting the empirical relationships implemented in the network model of gross gains, losses, and hydrologic turnover. Data points from this study exhibited high tracer velocities for a given Q as compared to other published stream and river results, and were best fit by a power law regression (Figure 5c). Median tracer velocity versus Q_{LOSS} data from this study were best fit with a negative exponential decline model, where Q_{LOSS} decreased as median tracer velocity increased (Figure 5d). During repeated mass recovery experiments, Q_{LOSS} varied with respect to both Q (Figure 5b) and median velocity (Figure 5d), indicating decreased %Loss as flow state increased.

3.3. Conceptual Network Model

[24] Our network model includes gross hydrologic gains and losses, hydrologic turnover, and discharge magnitude variability across the stream network (Figure 2). In our conceptualization, streamflow begins at the first reach in the network (R_1) when the threshold watershed contributing area necessary for stream channel initiation (~20 ha in this watershed) has been reached. Accordingly, R_1 does not have contributions from an upstream reach and is only subject to gains and losses across the reach. The output from R_1 (i.e., Q_1) becomes the input to the downstream reach (R_i), and additionally, gross hydrologic gains and losses

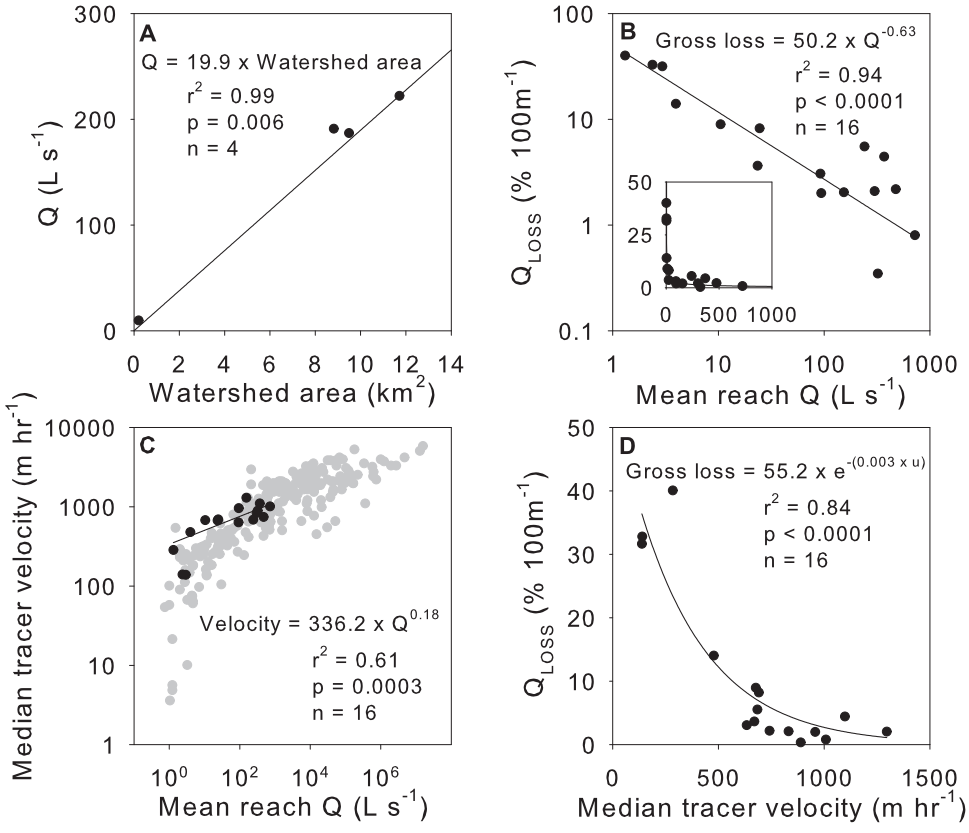

Figure 5. Regression relationships between (a) watershed area and stream discharge for 24 July 2006 (Q); (b) mean reach Q and gross loss (Q_{LOSS}); (c) mean reach Q and median tracer velocity for this study and 241 data points compiled from *Wondzell et al.* [2007], with power law fit to the Q and velocity data from this study; and (d) median tracer velocity and Q_{LOSS}.

occur across R_i. The sum of the input to R_i from the upstream reach and the gains and losses across R_i becomes the output from R_i (i.e., Q_i) and the input to the next downstream reach R_{i+1}. This process continues iteratively moving downstream to the watershed outlet (R_n), resulting in hydrologic turnover and heterogeneity in source water contributions and resulting stream water composition moving downstream (Figure 2).

3.4. Numerical Network Model

[25] We highlight four locations along the stream network (Figure 6a I–IV) illustrating the number of reaches (i.e., 10 m cells) in each upstream distance class (see bars in Figure 6b), and the variability in stream network structure upstream of each location. At the headwater site I, the upstream distance classes are fairly equally represented as indicated by the relatively flat distribution in Figure 6b I. Moving downstream to sites II and III (Figure 6b II, III), multimodal distributions are evident due to tributaries entering the stream network. At the watershed outlet (site IV) the distribution of distance classes more closely resembles a Gaussian distribution with the largest proportion of 10 m reaches located ~2750 m from the network outlet (Figure 6b IV). Lateral inflows from different upstream distance classes throughout the network are represented with bars in Figure 6c I–IV. At the headwater site I, the majority of lateral inflow is contributed at the stream channel initiation locations (i.e., channel heads, Figure 6c I). Moving downstream to sites II and III the distributions of lateral inflows become more heterogeneous with large lateral inflows at stream channel initiation sites and highly convergent hillslopes (Figure 6c II, III). The distribution of lateral inflows at the watershed outlet (site IV) more closely resembles a Gaussian distribution than the other highlighted locations and large lateral inputs are evident at locations ~2800 m upstream of the outlet (Figure 6c I).

[26] The percent contribution to Q from different upstream distance classes is shown as black lines in Figures 6b and 6c. Moving downstream from sites I to IV, peaks in contributions to Q are attenuated and there is an increasing influence of nearby contributions on downstream water composition (Figures 6b and 6c). The distribution of percent Q contribution at site I indicates that headwater streams are dominated by discrete, stream channel initiation inputs (Figures 6b and 6c I). At sites II and III contributions to Q from channel heads are diminished relative to the magnitude of channel head inputs at site I (Figures 6b and 6c). This trend continues moving downstream, and discrete inputs to Q at site IV are attenuated and larger proportional contributions to Q from relatively closer upstream locations are evident (Figures 6b and 6c).

[27] The influence of variable stream gains and losses, and network structure on source water contribution, stream water composition, and Q magnitude moving downstream along the main stem of the network are illustrated as spectra of flow source locations at each point along the main

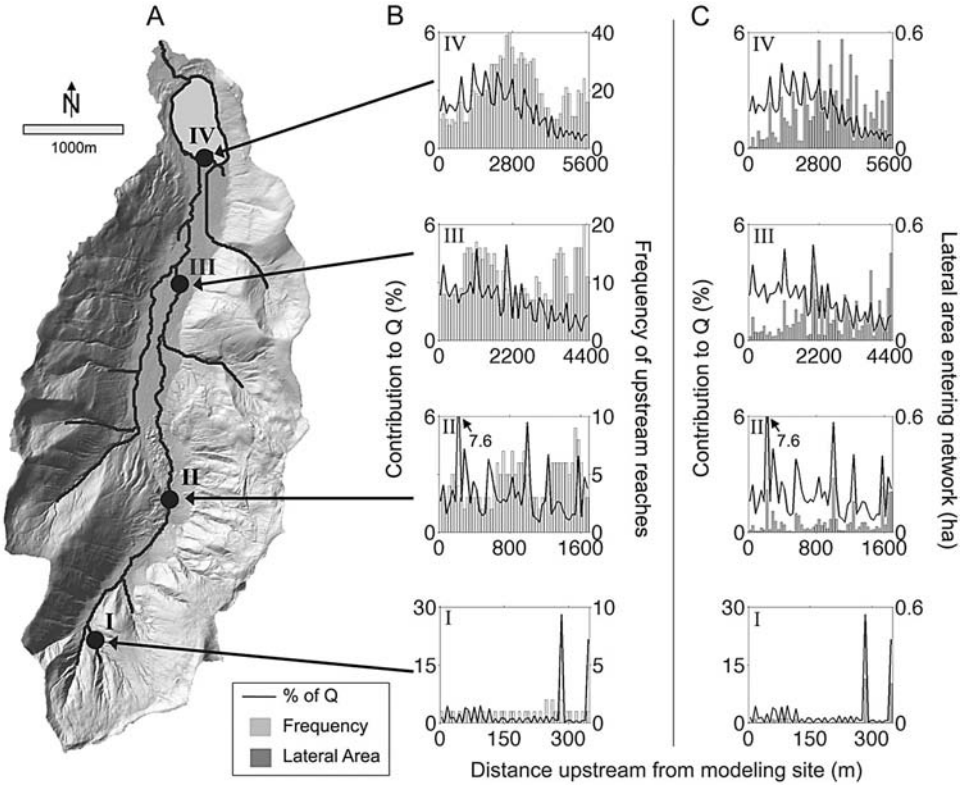

Figure 6. (a) Bull Trout stream network with four highlighted locations; (b) % contribution to Q and frequency of upstream 10 m reaches for the four locations; and (c) contribution to Q and lateral area entering the network upstream of the four locations.

stem of the stream network (Figure 7). Each color indicates a contribution to Q over each 10 m reach (Figure 7) that subsequently decays in a downstream direction as a function of the Q_{LOSS} equation presented in Figure 5b. Simultaneously, additional GW inputs contribute to streamflow as a function of increasing UAA following the relationship between watershed area and Q (see Figure 5a). Large increases in Q are due to tributary junctions (Figure 7). This turnover process results in increasingly heterogeneous stream water mixtures in the downstream direction (Figure

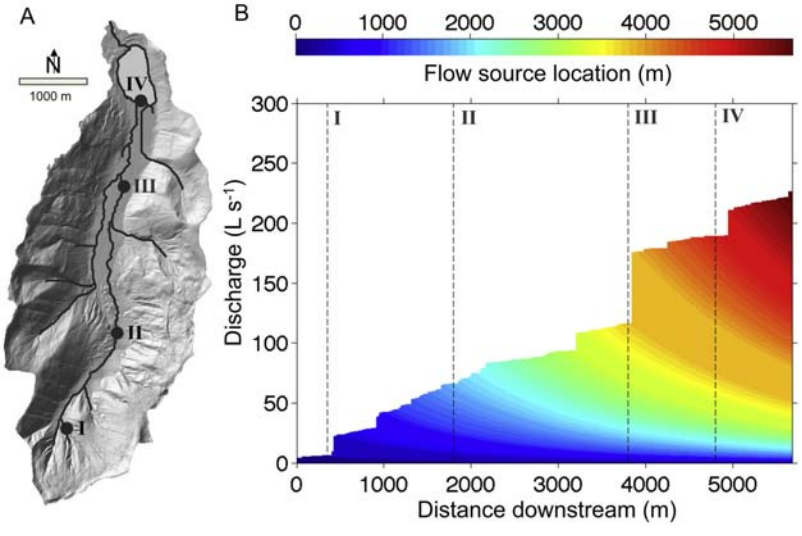

Figure 7. (a) Bull Trout stream network with four highlighted locations; and (b) source water contributions and resulting stream water composition and discharge magnitude moving downstream along the network. Each color represents input of different water along each 10 m stream reach.

7) and decreased influence of GW input from greater distances. This is evident in the stream water composition at site IV where source water contributions from headwater locations comprise a small percentage of Q at the watershed outlet (dark blue source water contribution to Q at site IV Figure 7). Additionally, the relative importance of any single input becomes muted moving downstream as increasingly more and more contributions are collected, mixed, and subjected to gain and loss (Figure 7). Together, these results demonstrate the importance of variable gains and losses, watershed structure, and network geometry in influencing stream water composition and Q magnitude across stream networks.

4. Discussion

4.1. How Do Magnitudes of Reach Scale Stream-GW Exchange Vary Across the Stream Network?

[28] Our results indicate that stream gains and losses occurred in the Bull Trout Watershed across a range of stream morphologies, sizes, flow states, and positions within the network regardless of whether the reach was net gaining or losing or the magnitude of net differences. These results demonstrate that streams do not simply gain or lose water as they flow downstream. In fact, the net changes in Q observed along the stream network are the result of gross gains and losses that occur sequentially or simultaneously along reaches (Figure 3).

[29] Medium to larger-sized streams were the sites of the largest volumetric exchanges between streams and groundwater (Figure 3). At the spatial scale of this study (i.e., lower order streams) these high volumetric exchanges can have strong impacts on streamflow magnitude, GW recharge, and aquifer storage state. Our temporally replicated experiments also indicated that these exchange processes were variable across flow states (Figure 3, Table 1). Specifically, the magnitude and direction of NetΔQ (i.e., net gain or net loss) was dependent on the interaction between flow state and groundwater storage status (Figure 5). Furthermore, exchange varied with respect to Q magnitude and Q_{LOSS} decreased with increased flow state (Figure 5). Additionally, we will note that these experiments occurred at base flow to high-base flow conditions, which may represent periods of high exchange relative to peak flow states [*Wondzell*, 2011]. It could be expected that Q_{LOSS} would continue to decrease along the trajectory shown in Figure 5b with increasing Q. Conversely, there could be very strong losses under drought conditions or in very arid environments. However, additional research to investigate relationships between Q, gross gain, gross loss, and resulting hydrologic exchange is necessary to understand these dynamics across spatial scales and hydroclimatic gradients.

[30] The exchanges that occurred in headwater tributaries (lower order streams) were of smaller volumetric magnitude than in higher order streams; however, when normalized by watershed area strong exchanges were observed in headwater streams (Figure 3e). Furthermore, the strong exchanges in smaller headwater streams resulted in high rates of fractional hydrologic turnover, despite less volumetric exchange compared to larger streams. Headwater streams have previously been noted as exerting important influences on watershed export and retention of nutrients [e.g., *Alexander et al.*, 2007; *Peterson et al.*, 2001], and our physical hydrology results support those findings. Specifically, in this study, headwater streams were found to be active sites of exchange; a process that has been suggested to be important in biogeochemical processing [*Mulholland et al.*, 1997] and nutrient transport and retention [*Covino et al.*, 2010; *Triska et al.*, 1989].

[31] Gains and losses can have strong influences on solute signatures and stream water composition (Figures 3f and 7). For example, across reaches 2, 3, and 4 exchanges were ~20%–40% 100 m^{-1} (Figure 3f); exchanges of this magnitude could impact solute signatures over relatively short stream distances, potentially "resetting" stream water chemistry [*Covino and McGlynn*, 2007] with strong implications for both solute transport and interpretation of solute data (Figure 3f, Figure 7).

[32] NetΔQ was highly variable across the stream network (Figures 3g–3i). Smaller reaches were typically net losing, medium sized reaches were net gaining, and the largest reaches were temporally variable (Figures 3g–3i). However, across all of these different net gaining and losing reaches we observed both gross gains and gross losses. Furthermore, we observed patterns related to gains, losses, and Q across the landscape (Figure 5) that we were able to take advantage of and implement in our numerical network model. These hydrologic dynamics were related to landscape position and flow state, and when combined with network organization/structure helped to elucidate controls over spatial source water contributions to Q and stream water compositions across the watershed. Taken together, these empirical results suggest quantifying reach gains and losses across all stream sizes can provide: (1) a more complete understanding and assessment of stream-GW exchange than NetΔQ alone; and (2) insight into how these exchange dynamics influence stream water composition, Q magnitude, GW storage state, and solute transport.

4.2. How Do Observed Reach Scale Stream-GW Exchange and Hydrologic Turnover Processes Combine to Influence Source Water Contributions and Stream Water Composition at the Network Scale?

[33] We developed a conceptual model that integrates variable gains, losses, and fractional hydrologic turnover (serial processing) along a stream network to investigate how these processes, combined with watershed structure and network geometry, influence source water contributions, stream water composition, and solute transport moving downstream. The conceptual framework is simple and accounts for upstream input, gains and losses across the reach, and downstream output (Figure 2). GW input coupled with loss of stream water to the GW system across each reach led to hydrologic turnover, or the fractional turnover of stream water, which resulted in spatially variable stream water composition (Figures 6 and 7).

[34] Our model simulated network source water contributions and hydrologic turnover that led to stream water composed of water from numerous sources over distances of a few km (Figures 6 and 7). The influence of any one source diminished moving downstream along the network because of the fractional turnover process and increasing in-stream volume and number of source waters (Figure 7). The composition of the resulting mixture at any point in the stream network is a function of watershed structure, with

strong gains resulting from large lateral inflows associated with highly convergent areas, and fractional loss. Because the stream water loss is fractional, each GW input signature is diminished with distance downstream, though never fully erased. Quantifying contributions from spatially distinct watershed locations (i.e., lateral inflows) and their proportional influences on signatures across the network and at the watershed outlet provides new insight into streamflow generation and what a stream sample or observation might reflect.

[35] Our numerical network model allowed us to investigate the relationships between (1) watershed structure and the arrangement of GW input across the network, (2) the hydrologic turnover process that coupled with GW inputs control stream water composition, and (3) the proportional influences of source water contributions to stream water composition along the network and at the watershed outlet (Figures 6 and 7). Our results demonstrate that the relationship between percent contribution to Q and number of upstream 10 m reaches (network geometry) and upstream contributing areas (watershed structure) changes moving downstream (Figure 6). Figures 6b I and 6c I demonstrate that in the headwater regions the percent contribution to Q is strongly related to both number of upstream 10 m reaches (Figure 6b I) and lateral contributing area (Figure 6c I). This suggests that Q in the headwaters is closely linked to local hillslopes and/or runoff generation processes. However, closer to the watershed outlet this relationship changes and other features of the watershed/stream network structure have greater influence on stream water composition. For instance, while peaks in the distribution of contribution to Q do indeed correspond to larger lateral area and larger GW inputs, and the arrangement of these lateral inflows is related to watershed structure (Figure 6), the distribution of percent contribution to Q becomes increasingly decoupled from the distribution of upstream reaches (Figure 6b) and lateral inflow (Figure 6c) moving from headwaters to watershed outlet locations. This highlights the influence network geometry exerts over stream solute composition and proportional source water contributions from across spatial distance classes. Furthermore, this indicates that contributions to Q change strongly moving downstream from being dominated by stream channel initiation contributions at site I (i.e., headwater), to larger proportional contributions from relatively closer spatial locations and decreased importance of headwater inputs at site IV (Figure 6b). Although peaks in contribution to Q indicate large inputs of water at tributaries and highly convergent hillslopes, these peaks become increasingly attenuated and decoupled from the corresponding peaks in lateral area moving downstream toward the outlet (Figure 6c IV). This decoupling suggests a conversion from hillslope to watershed/stream network control of source water contributions and stream water composition moving from headwater to watershed outlet stream reaches.

[36] These modeling results indicate that stream water composition at a given location is controlled, at least in part, by the structure of the upstream watershed and channel network and their influences on variable gains, losses, and hydrologic turnover. Our results suggest that water samples collected at watershed outlets do not equally integrate signals from within the watershed, but rather represent a variable integration weighted by hydrologic turnover and the spatial organization of where water initially enters the network (i.e., GW input). Given that watershed studies often take advantage of outlet samples or stream network synoptic sampling to infer processes, this study indicates that it is important to understand and recognize the implications of watershed structure, network geometry, and hydrologic turnover dynamics on influencing the proportional influences various regions of the landscape impart on the integrated signals observed along networks and at watershed outlets.

4.3. Management Implications

[37] Hydrologic turnover has important implications for management applications such as contaminant transport, nutrient transport, and surface and GW quality. Transient storage models (TSMs) have often been used to simulate solute tracer movement, stream-GW exchange, and subsequent downstream transport. While TSMs have provided a very useful context for interpreting stream tracer data and for developing estimates of downstream transport of solutes, contaminants, and nutrients, the exchanges outlined here incorporate larger scales and longer residence time GW flow domains than typical to TSMs. Furthermore, TSM parameterizations have generally been constrained using only recovered tracer breakthrough curve (BTC) data, which neglects any gross loss (e.g., mass loss due to lateral outflow) to GW systems, and potentially influences estimates of solute transport (e.g., residence time estimates). Indeed, *Szeftel et al.* [2011] noted that stream-GW exchanges are difficult to elucidate from NetΔQ data alone and demonstrated that gain (lateral inflow) and loss (lateral outflow) dynamics can impact TSM parameter estimates and interpretation of stream tracer BTCs. Expanding our conceptual understanding to include longer residence time flow paths could help improve estimates of the movement and export of solutes (contaminants, nutrients, or other) across and from watersheds. Additionally, incorporating larger scale stream-GW exchanges and hydrologic turnover into conceptual and numerical network models has strong potential to enhance not only basic understanding of watershed processes but also to provide valuable tools to aid decision making in land and watershed management situations.

5. Summary

[38] We presented field-based and numerical network modeling results of: hydrologic gains, losses, and fractional turnover; source water contributions and stream water compositions across the network; and the influence watershed structure and network geometry exert over source water contributions and stream water compositions. We observed gross gains and losses across all reaches of various types (e.g., headwater to valley bottom) and sizes (first–third order, 0.8–730.4 L s^{-1}) within the Bull Trout Watershed regardless of whether the reach was net gaining or losing, or the magnitude of the net change in Q across the reach. We also observed strong relationships between gross loss (Q_{LOSS}) and Q, and gross gain (Q_{GAIN}) and watershed contributing area, that we implemented in our numerical network model of fractional hydrologic turnover to scale these processes spatially across the stream network. These combined field and model-based results indicated

that stream water composition was dominated by hillslope (i.e., stream channel initiation) contributions in the headwaters, whereas network geometry and hydrologic turnover controlled stream water composition near the watershed outlet. We assessed the relationships between watershed structure, network geometry, and source water contributions and stream water compositions across the network and found a decoupling between where GW inputs enter the network and their proportional influences on solute signatures or Q magnitude moving toward the outlet, or downstream along the network, due to the fractional turnover process. This suggests that the proportional influences on stream water composition are a function of both the location in the network where GW enters, the magnitude of that input, and the subsequent turnover process that diminishes the influence of the original input.

[39] In summary, we suggest that (1) net changes in Q may not properly characterize the hydrologic exchanges occurring along stream reaches, (2) gross hydrologic gains and losses combine to control net changes in Q and are controlled by watershed structure and network geometry, (3) these gains and losses lead to hydrologic turnover, which can have important implications for source water contributions, stream water composition, Q magnitude, and GW recharge and aquifer storage state, (4) this hydrologic turnover process should be incorporated into future hydrological, solute transport, and biogeochemical network models, and (5) these analyses helped to unravel the internal mechanisms that partially control the hydrological and biogeochemical signals observed along stream networks and at watershed outlets.

[40] **Acknowledgments.** Financial support was provided by grants from the National Science Foundation DEB-0519264 (to MT State University), and an Environmental Protection Agency (EPA) STAR Fellowship awarded to Covino. We would like to thank Brian Iacona, Kelly Conde, Malcolm Herstand, and Alexey Kalinin for assistance with fieldwork. We thank the Boise National Forest for allowing access to sampling sites.

References

Alexander, R. B., E. W. Boyer, R. A. Smith, G. E. Schwarz, and R. B. Moore (2007), The role of headwater streams in downstream water quality, *J. Am. Water Resour. Assoc.*, *43*(1), 41–59.

Cardenas, M. B. (2008), Surface water-groundwater interface geomorphology leads to scaling of residence times, *Geophys. Res. Lett.*, *35*, L08402, doi:10.1029/2008GL033753.

Covino, T. P., and B. L. McGlynn (2007), Stream gains and losses across a mountain to valley transition: Impacts on watershed hydrology and stream water chemistry, *Water Resour. Res.*, *43*, W10431, doi:10.1029/2006WR005544.

Covino, T., B. McGlynn, and M. Baker (2010), Separating physical and biological nutrient retention and quantifying uptake kinetics from ambient to saturation in successive mountain stream reaches, *J. Geophys. Res.*, *115*, G04010, doi:10.1029/2009JG001263.

Grabs, T. J., K. G. Jencso, B. L. McGlynn, and J. Seibert (2010), Calculating terrain indices along streams: A new method for separating stream sides, *Water Resour. Res.*, *46*, W12536, doi:10.1029/2010WR009296.

Harvey, J. W., B. J. Wagner, and K. E. Bencala (1996), Evaluating the reliability of the stream tracer approach to characterize stream-subsurface water exchange, *Water Resour. Res.*, *32*(8), 2441–2451.

Jencso, K. G., B. L. McGlynn, M. N. Gooseff, S. M. Wondzell, K. E. Bencala, and L. A. Marshall (2009), Hydrologic connectivity between landscapes and streams: Transferring reach and plot scale understanding to the catchment scale, *Water Resour. Res.*, *45*, W04428, doi:10.1029/2008WR007225.

Kiilsgaard, T., L. Stanford, and R. Lewis (2003), Preliminary geologic map of the northeast part of the Deadwood River 30 × 60 minute quadrangle, Idaho, *Idaho Geologic Survey*, Moscow, Idaho.

Kilpatrick, F. A., and E. D. Cobb (1985), Measurement of discharge using tracers, *Report of the U.S. Geological Survey, Techniques of Water-Resources Investigations*, Book 3, Chap. A16, U.S. Geol. Survey.

McGlynn, B. L., and J. Seibert (2003), Distributed assessment of contributing area and riparian buffering along stream networks, *Water Resour. Res.*, *39*(4), 1082, doi:10.1029/2002WR001521.

Mulholland, P. J., E. R. Marzolf, J. R. Webster, D. R. Hart, and S. P. Hendricks (1997), Evidence that hyporheic zones increase heterotrophic metabolism and phosphorus uptake in forest streams, *Limnol. Oceanogr.*, *42*(3), 443–451.

O'Callaghan, J. F., and D. M. Mark (1984), The extraction of drainage networks from digital elevation data, *Comput. Vision Graphics Image Processing*, *28*(3), 323–344.

Payn, R. A., M. N. Gooseff, B. L. McGlynn, K. E. Bencala, and S. M. Wondzell (2009), Channel water balance and exchange with subsurface flow along a mountain headwater stream in Montana, United States, *Water Resour. Res.*, *45*, W11427, doi:10.1029/2008WR007644.

Peterson, B. J., et al. (2001), Control of nitrogen export from watersheds by headwater streams, *Science*, *292*(5514), 86–90.

Ren, J. H., and A. I. Packman (2005), Coupled stream-subsurface exchange of colloidal hematite and dissolved zinc, copper, and phosphate, *Environ. Sci. Technol.*, *39*(17), 6387–6394.

Ruehl, C., A. T. Fisher, C. Hatch, M. Los Huertos, G. Stemler, and C. Shennan (2006), Differential gauging and tracer tests resolve seepage fluxes in a strongly-losing stream, *J. Hydrol.*, *330*(1–2), 235–248.

Schmadel, N. M., B. T. Neilson, and D. K. Stevens (2010), Approaches to estimate uncertainty in longitudinal channel water balances, *J. Hydrol.*, *394*(3–4), 357–369.

Seibert, J., and B. L. McGlynn (2007), A new triangular multiple flow direction algorithm for computing upslope areas from gridded digital elevation models, *Water Resour. Res.*, *43*, W04501, doi:10.1029/2006WR005128.

Story, A., R. D. Moore, and J. S. Macdonald (2003), Stream temperatures in two shaded reaches below cutblocks and logging roads: Downstream cooling linked to subsurface hydrology, *Can. J. For. Res.*, *33*(8), 1383–1396.

Szeftel, P., R. D. Moore, and M. Weiler (2011), Influence of distributed flow losses and gains on the estimation of transient storage parameters from stream tracer experiments, *J. Hydrol.*, *396*(3–4), 277–291.

Triska, F. J., V. C. Kennedy, R. J. Avanzino, G. W. Zellweger, and K. E. Bencala (1989), Retention and transport of nutrients in a 3rd order stream in northwestern California—Hyporheic processes, *Ecology*, *70*(6), 1893–1905.

Woessner, W. W. (2000), Stream and fluvial plain ground water interactions: Rescaling hydrogeologic thought, *Ground Water*, *38*(3), 423–429.

Wondzell, S. M. (2011), The role of the hyporheic zone across stream networks, *Hydrol. Processes*, *25*, 3525–3532, doi:1010.1002/hyp.8119.

Wondzell, S. M., M. N. Gooseff, and B. L. McGlynn (2007), Flow velocity and the hydrologic behavior of streams during baseflow, *Geophys. Res. Lett.*, *34*, L24404, doi:10.1029/2007GL031256.

T. Covino, J. Mallard, and B. McGlynn, Department of Land Resources and Environmental Sciences, Montana State University, 334 Leon Johnson Hall, Bozeman, MT, USA. (tpcovino@gmail.com)